

Electronic Supplementary information

## Multi-modal optimization of bismuth vanadate photoanodes via combinatorial alloying and hydrogen processing

P. F. Newhouse, D. Guevarra, M. Umehara, D. A. Boyd, L. Zhou, J. K. Cooper, J. A. Haber, J. M. Gregoire

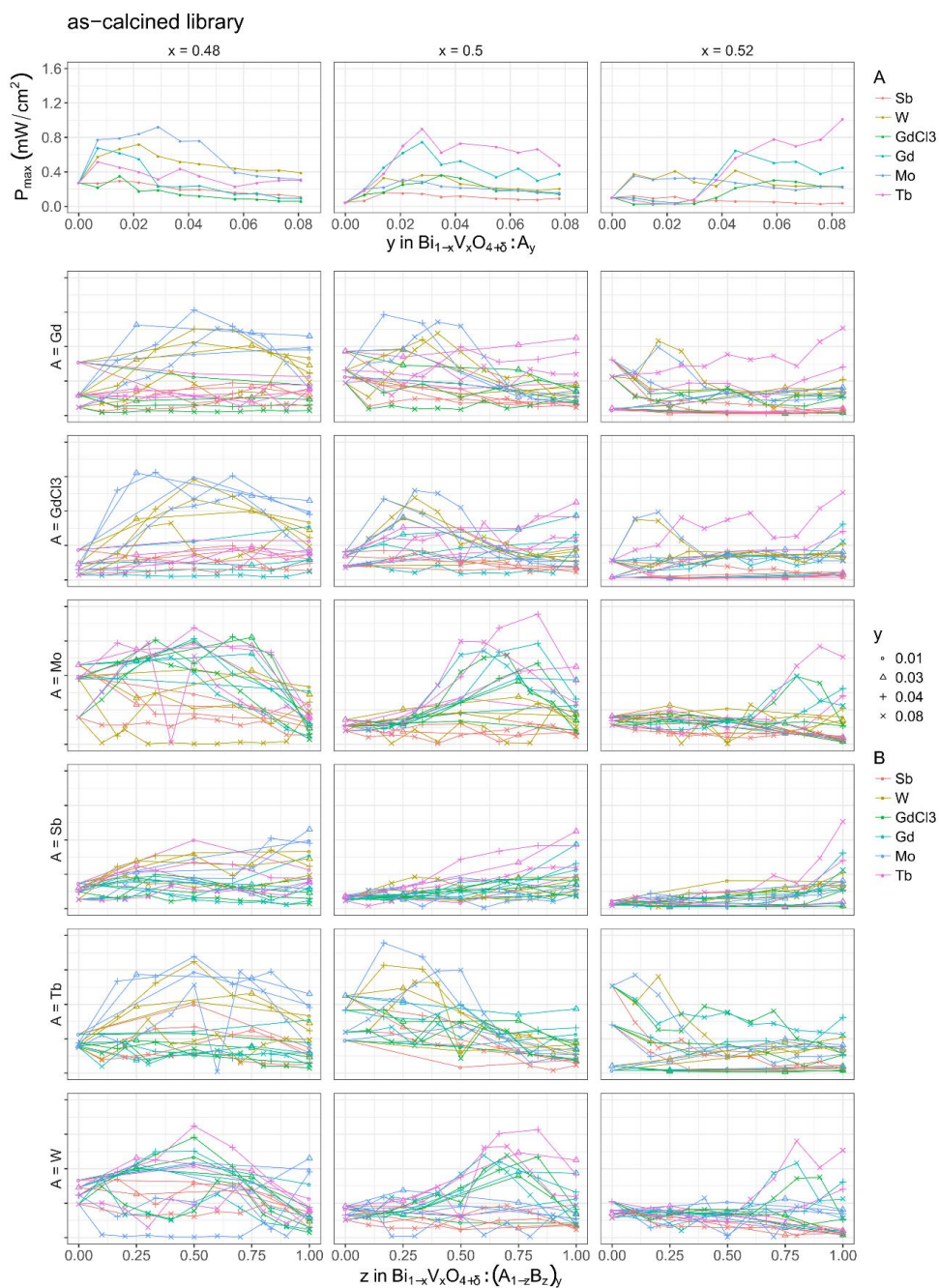


Figure S1a. Photoelectrochemical  $P_{max}$  measurements from approximately 1700 as-calcined BVO-based photoanodes alloyed with various amounts of A = Sb, W, Gd, Mo, or Tb (upper 3 panels) and their pairwise combinations (lower 18 panels). The vertical columns indicate the host  $\text{Bi}_{1-x}\text{V}_x\text{O}_4$  stoichiometry,  $\text{Bi}_{52}\text{V}_{48}$ ,  $\text{Bi}_{50}\text{V}_{50}$ , and  $\text{Bi}_{48}\text{V}_{52}$ . In the lower 18 panels,  $P_{max}$  values from co-alloyed Mo-Gd, Mo-Tb, and W-Tb samples exceed the performance of any singly alloyed composition and reveal a generalized co-alloying synergy between an electron donating transition metal (Mo or W) and a structure modulating rare earth element (Gd or Tb). Each non-end member data point in the lower 18 panels is a single data point, while each data point in the three upper panels is a median value of 5 duplicate compositions. Many co-alloyed samples in the  $x = 0.48$  column exhibit  $P_{max}$  values exceeding the 3-cation performance limit, but zircon-type  $\text{BiVO}_4$  was detected from many of these samples via x-ray diffraction (see figure S4) and subsequent analysis was restricted to alloyed  $\text{BiVO}_4$  showing only the monoclinic (clinobisvanite) phase, which exist in the  $x = 0.5$  column of panels. The  $x = 0.5$  column data are used in the x-axis of Figure 1b.

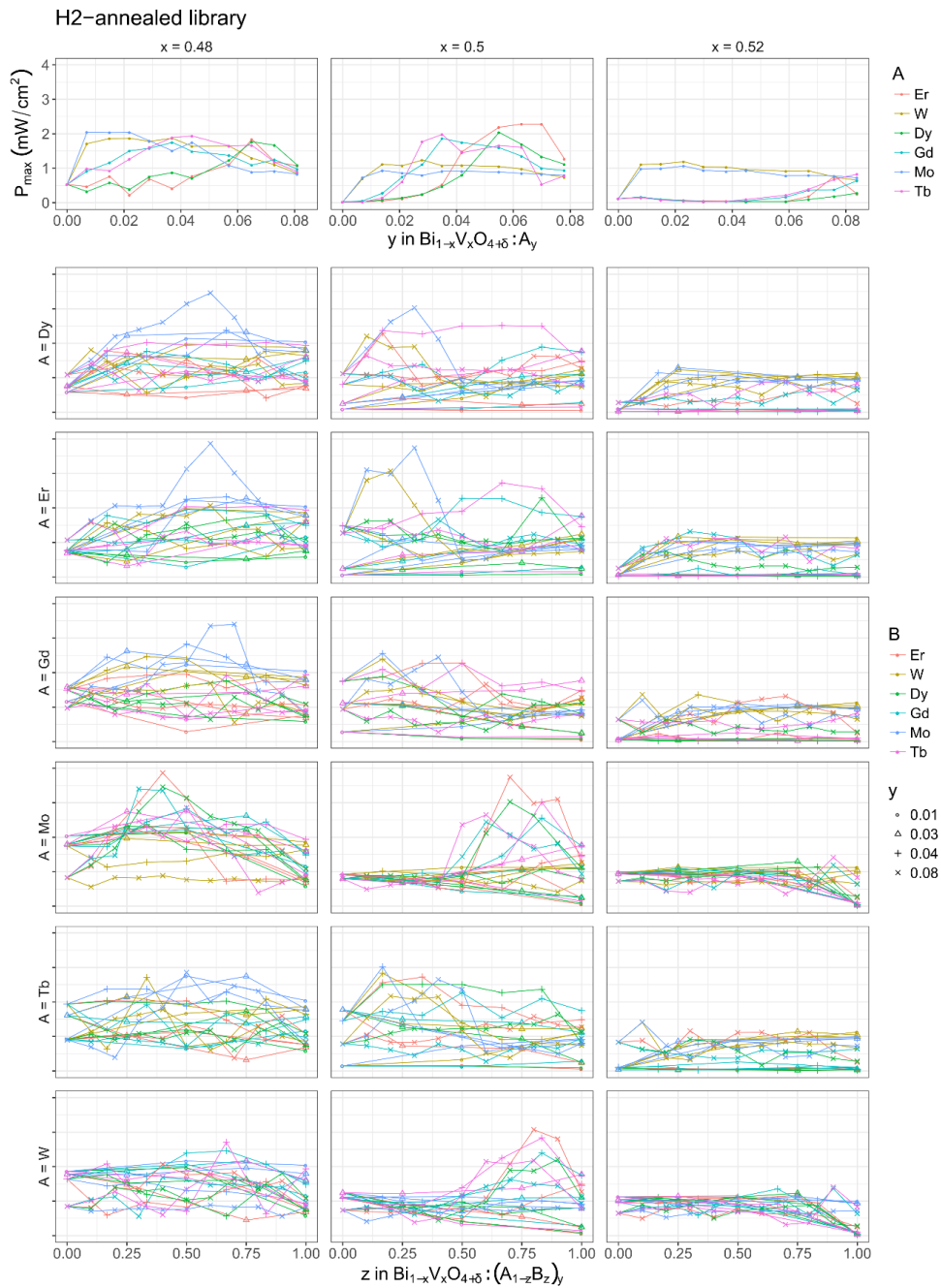


Figure S1b. Analogous to Figure S1a, photoelectrochemical  $P_{max}$  data from an H<sub>2</sub>-annealed, BiVO<sub>4</sub>-based combinatorial library alloyed with Er, W, Dy, Gd, Mo, and Tb. The y-axis range is larger than Figure S1a on account of the performance enhancement upon H<sub>2</sub> annealing. The  $x = 0.5$  column data are used in the y-axis of Figure 1b.

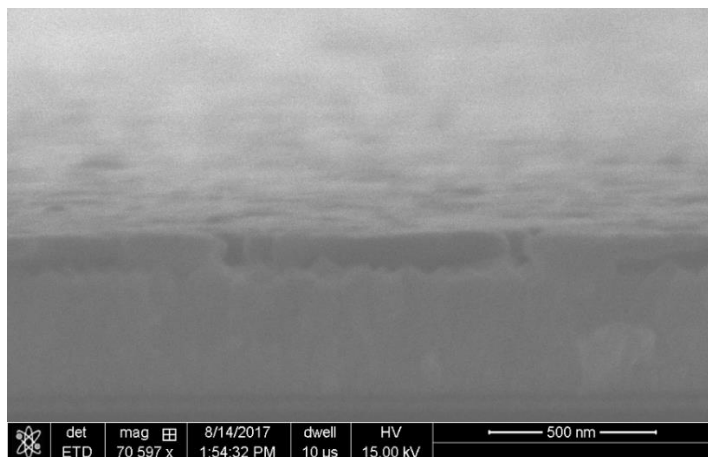


Figure S2. A cross sectional SEM image of an ink jet prepared,  $\text{BVO}_4$ -based photoanode on FTO-coated glass exhibiting a thickness of about 100 nm. This thickness value is considered to be representative of all  $\approx 1700$  samples in the library since the total (host + alloy) molar loadings of each sample are approximately equal.

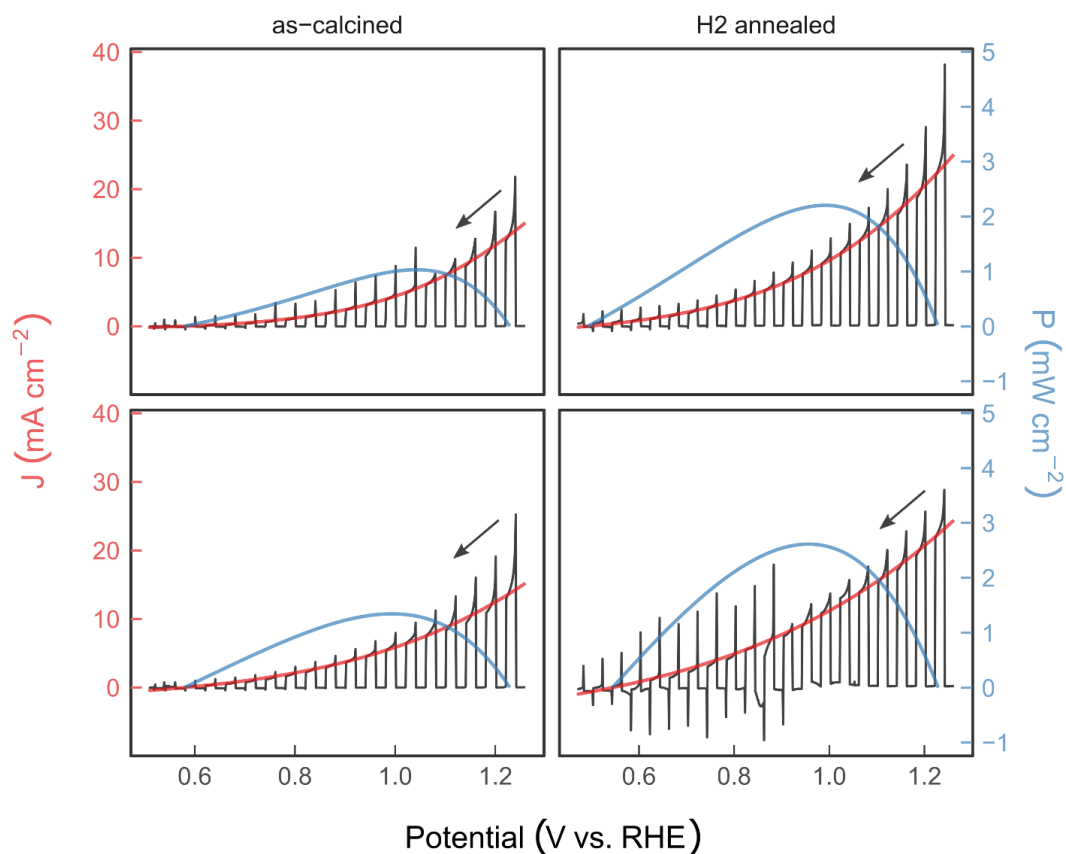


Figure S3. Cathodic, chopped illumination CV sweeps of the high performing samples from Figure 1a with the fitted photocurrent density (red) and power generation (blue) traces. The arrows indicate the sweep direction, beginning at 1.26 V vs. RHE and sweeping down to 0.51 V at  $20 \text{ mV s}^{-1}$ .

## Comment on zircon-type $\text{BiVO}_4$ detected from combinatorial libraries

An observation from x-ray diffraction measurements that we did not pursue is that some high-performing Bi-rich compositions ( $x = 0.48$ ) contained the zircon (pucherite) polymorph of  $\text{BiVO}_4$ <sup>1, 2</sup> and monoclinic (clinobisvanite)  $\text{BiVO}_4$  that has been the primary focus for PEC applications, prompting our exclusion of these Bi-rich compositions for any possible scale up or characterization efforts (Figure S3, below).

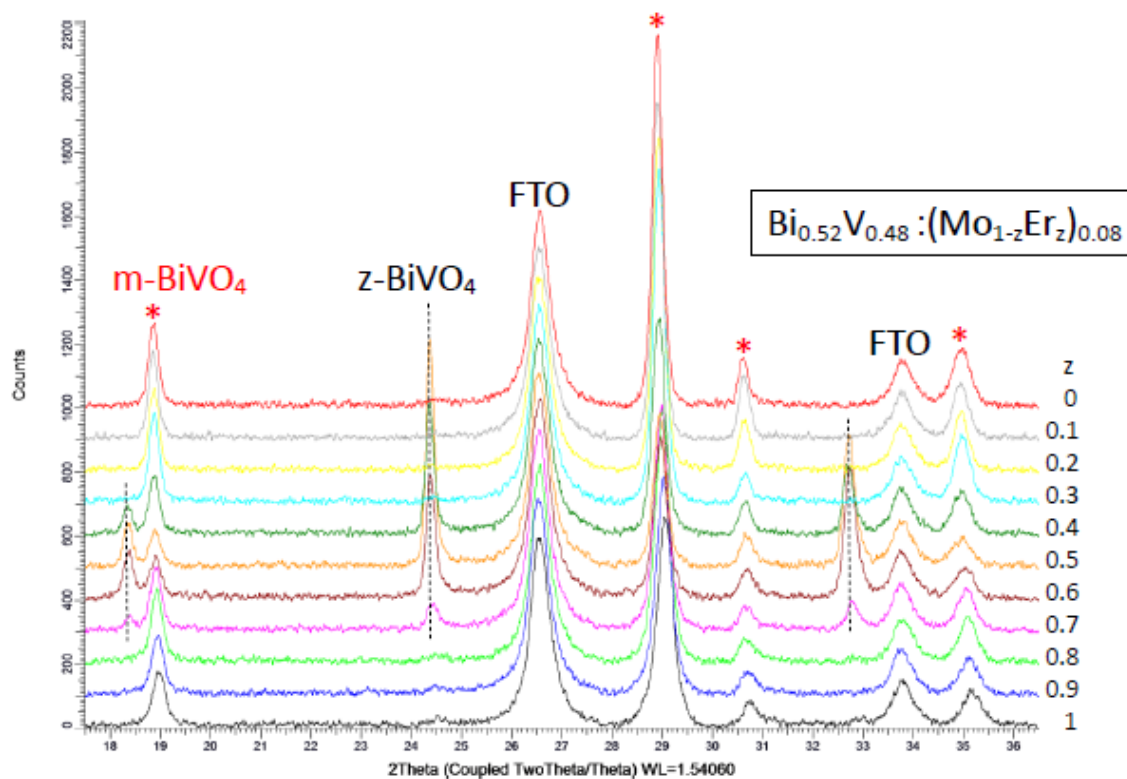


Figure S4. Stacked x-ray diffraction patterns from the 11 samples of composition  $\text{Bi}_{52}\text{V}_{0.48}:(\text{Mo}_{1-z}\text{Er}_z)_{8\%}$ ,  $0 \leq z \leq 1$  [analogous behavior was observed for the other (Mo,RE) sets]. Peaks from monoclinic BVO are indicated by a red asterisk while peaks from zircon BVO are indicated by a dashed vertical line.

Characterization of scaled up photoelectrodes (figures S5-S9, S11)

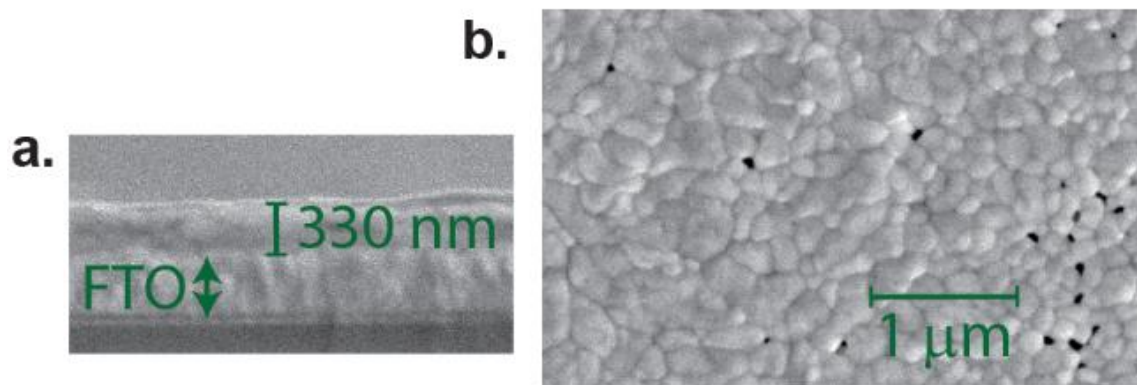


Figure S5. Cross sectional (a) and surface (b) SEM images of the Bi-V-Mo-Gd scaled up electrode in Figure 2. 50-100 nm pores can be seen in (b).

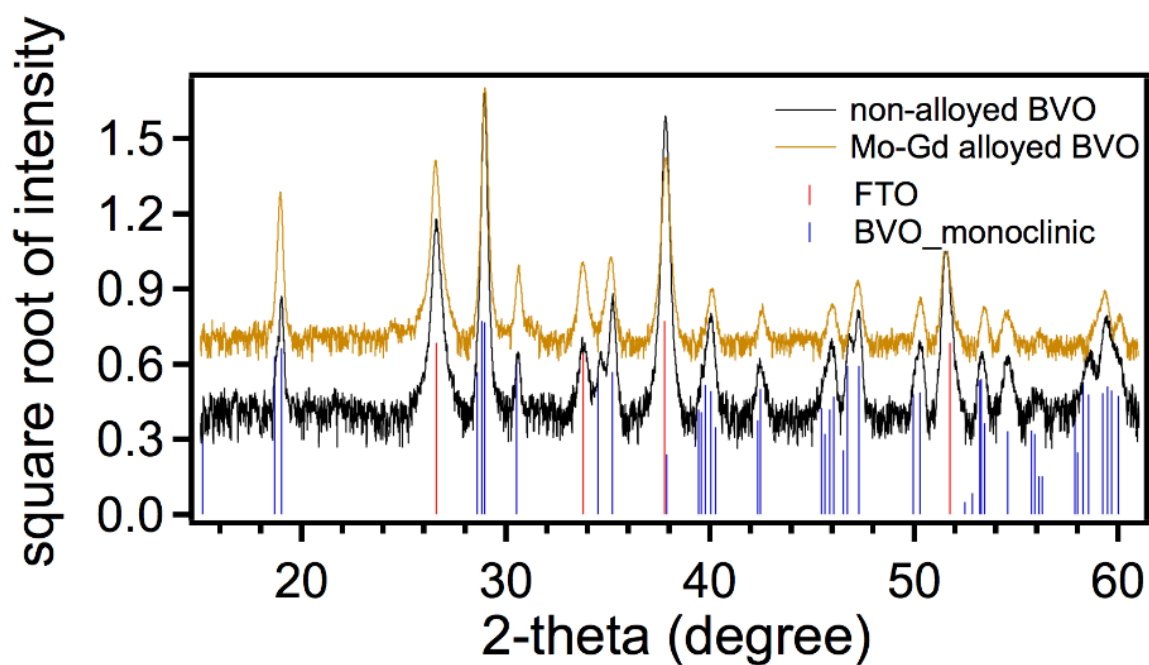


Figure S6. XRD patterns from the Mo-Gd and non-alloyed photoelectrodes from Figure 2 exhibiting phase pure synthesis.

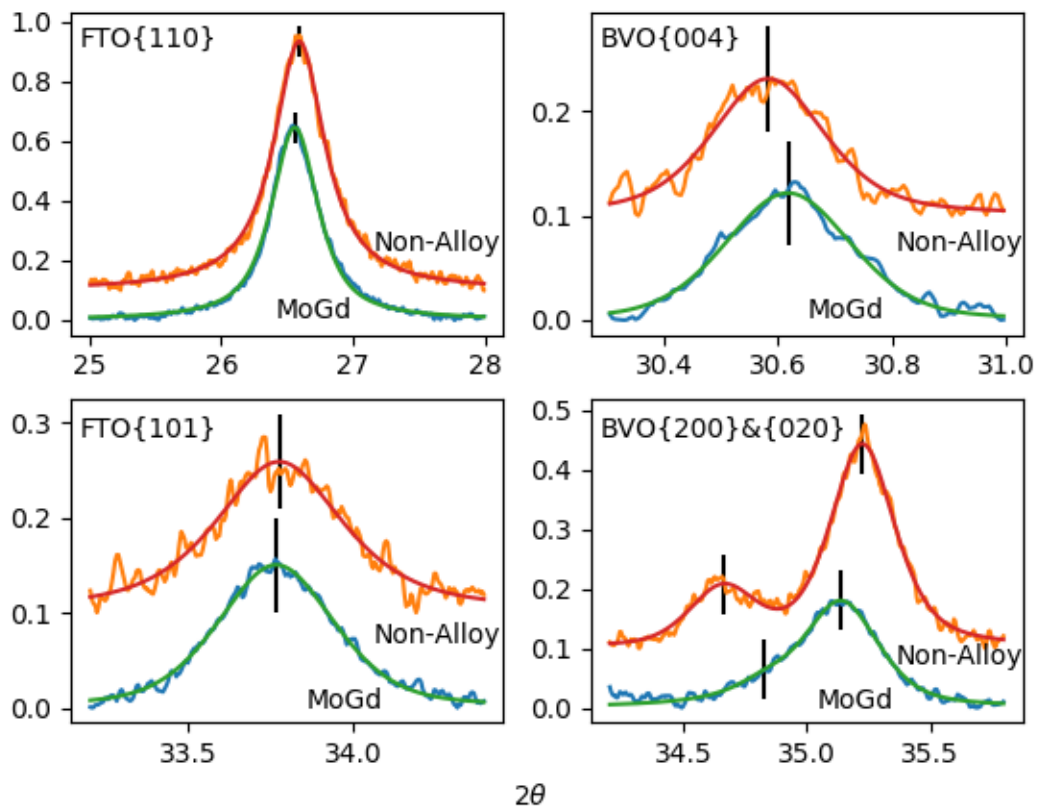


Figure S7. Fitted peak position and width from the {004} m-BVO diffraction peak from Figure S6. Debye Scherrer analysis indicates that both the non-alloyed sample and the MoGd sample have grain size of approximately 30 nm. Considering the BVO 004 peak width, the MoGd sample has about 10% smaller grain size than the non-alloy sample, or approximately 30% smaller grain size when additionally using FTO as an internal standard.

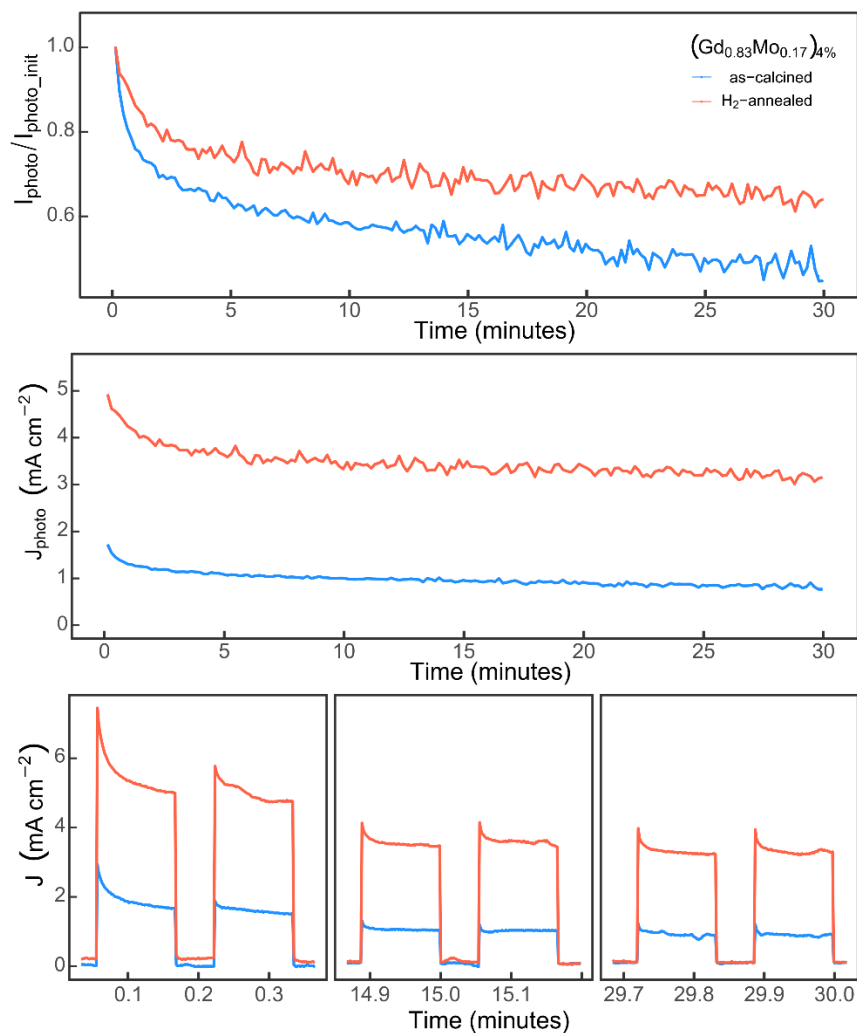


Figure S8. Photocurrent density vs. time of an optimized, scaled up Mo-Gd photoelectrode at  $V_{pmax}$  (0.94 V vs. RHE) before and after H<sub>2</sub> processing using chopped 455 nm ( $413 \text{ mW cm}^{-2}$ ) illumination in sulfite-free pH 7.2 phosphate buffer (middle and lowermost panels). The upper most panel shows the photocurrent decay normalized to the time = 0 photocurrent to visualize the relative stability of the 2 samples. After 10 minutes the H<sub>2</sub> processed sample has dropped to about 70% of its initial value, while the as-calcined sample has decayed to ~60% of the initial photocurrent and continues dropping further.

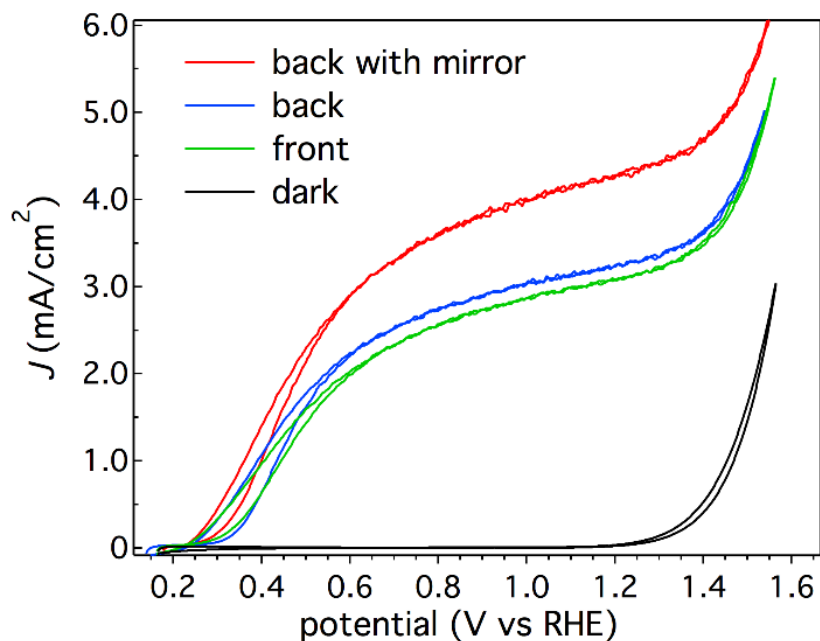


Figure S9. AM 1.5 photocurrent density for the scaled up Bi-V-Mo-Gd sample from Figure 2 under front, back, and back illumination with a Ag mirror to reflect unabsorbed light. The 1.23 V vs. RHE photocurrent densities are  $3.1 \text{ mA cm}^{-2}$ ,  $3.3 \text{ mA cm}^{-2}$ , and  $4.3 \text{ mA cm}^{-2}$ , respectively.

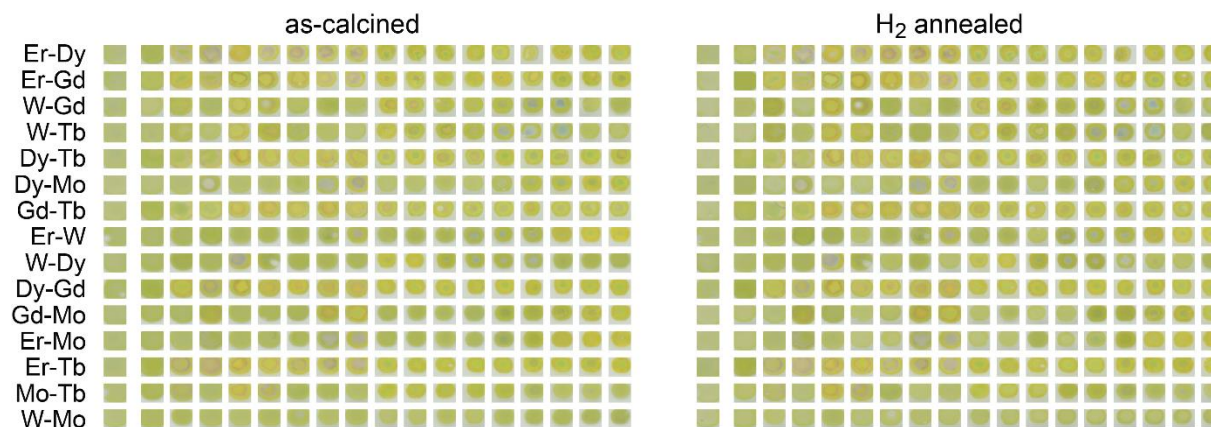


Figure S10. Cropped images of each co-alloy composition before and after  $\text{H}_2$  annealing, revealing no change in the apparent optical absorption. For each row of images, the left-most image is a duplicate non-alloy sample deposited among the respective co-alloy samples, and the 17 co-alloy samples are also shown.

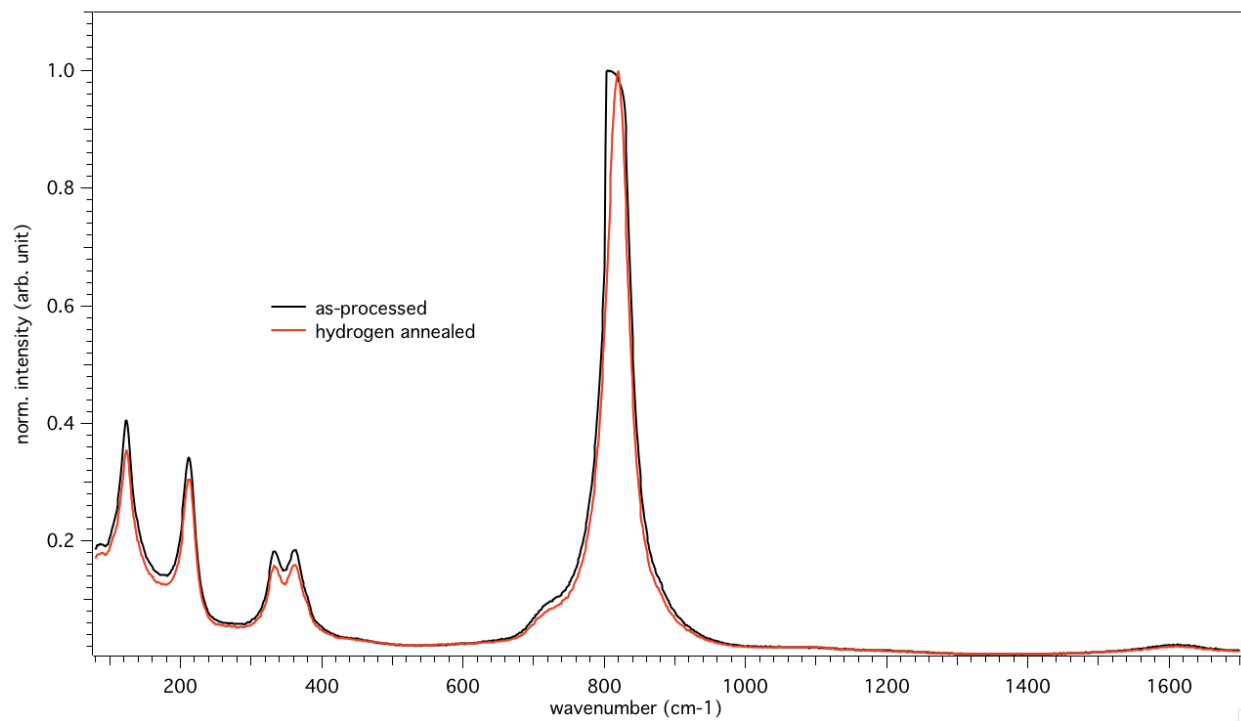


Figure S11. Raman spectra of an optimized scale up Bi-V-Mo-Gd sample before and after H<sub>2</sub> annealing showing no significant change, in agreement with main paper reference 20.

## References

1. A. Kudo, K. Omori and H. Kato, *Journal of the American Chemical Society*, 1999, **121**, 11459-11467.
2. S. Tokunaga, H. Kato and A. Kudo, *Chemistry of Materials*, 2001, **13**, 4624-4628.